Computation of reflector surfaces for bivariate beamshaping in the elliptic case

1976 J. Phys. A: Math. Gen. 9 2159

(http://iopscience.iop.org/0305-4470/9/12/020)

J. Phys. A: Math. Gen., Vol. 9, No. 12, 1976. Printed in Great Britain. © 1976

Computation of reflector surfaces for bivariate beamshaping in the elliptic case

A P Norris†§ and B S Westcott‡

† Plessey Radar Limited, Cowes, Isle of Wight PO31 8PF, UK
‡ Department of Mathematics, University of Southampton, Southampton SO9 5NH, UK

Received 5 April 1976, in final form 19 July 1976

Abstract. A numerical method for designing reflector surfaces that produce a specified far-field over a given solid angle when illuminated by an isotropic source is presented. The technique, which uses the geometrical optics approximation, requires the solution of a particular non-linear, elliptic partial differential equation, previously derived by the authors. The equation is solved iteratively by applying a finite difference model to a linearized form. Examples of some generated reflector surfaces are given showing the existence of two distinct solutions for each case. The method is applicable to problems in microwave antenna design, optics and acoustics.

1. Introduction

The geometrical optics approximation has been used extensively in the past twenty-five years in microwave design applications to synthesize reflector surfaces that produce a desired beam shape when illuminated by a particular primary feed.

Early beam-shaping techniques were directed towards producing shaped beams for search radar antennae (Dunbar 1948) and later work has mainly been concerned with shaping the reflecting surfaces of Cassegrain antennae in order to optimize performance (Galindo 1964). However, up until recently the function describing the beam shape has been required to be of only one variable. The advent of communications satellites has underlined the need for a more flexible design method, since in order to illuminate irregular regions of the earth efficiently, the satellite antenna must produce an appropriate beam shape to prevent 'spillover' into neighbouring regions (Millington 1975).

In a recent paper (Westcott and Norris 1975) the authors have laid the theoretical foundations of a method by which reflector surfaces are generated under the geometrical optics approximation, capable of producing a far-field specified as a function of two variables. The governing partial differential equations derived from the principle of energy conservation and the geometrical law of reflection can be either elliptic or hyperbolic.

Theoretical analysis and the subsequent computation of reflector surfaces in the hyperbolic case have been described in a parallel series of papers (Brickell and Westcott 1976, Westcott and Brickell 1976), where the problem is formulated as an initial-value problem.

§ Formerly with the Department of Mathematics, University of Southampton.

In this paper we consider the elliptic case only and indicate a numerical method which we have used successfully to generate reflector surfaces. The elliptical form of the equations is presented, for convenience, in § 2. It is shown that the reflector surface is realized by the solution of a non-linear second-order partial differential equation which is subjected to certain linear and non-linear boundary conditions. The non-linear equations are linearized for local perturbations in § 3 and a finite difference method for their solution is presented in § 4. Section 5 contains some computed results corresponding to two distinct far-field models. Our conclusions are given in § 6.

2. Design equations

It has been shown (Norris and Westcott 1974, Westcott and Norris 1975) that in order to synthesize a reflector surface fed from a point source and capable of giving a desired generalized far-field, a particular non-linear partial differential equation of the Monge–Ampère type must be solved. The geometry of the problem is shown in figure 1 and the relevant equations are included here for reference.

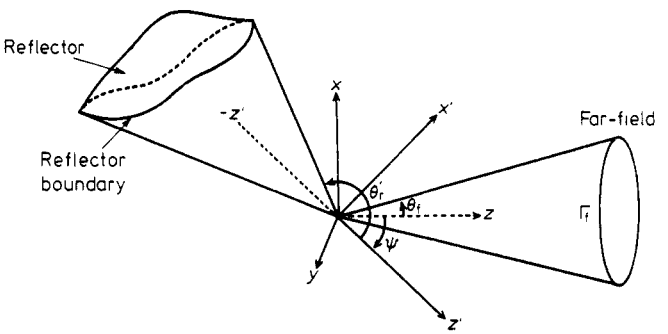

Figure 1. Geometry.

The required far-field power density function $G(\theta, \phi)$, which is essentially finite and positive, is defined on the surface of a sphere centred at the source point O, the origin for spherical polar coordinates. The primary source is considered to have a power density function $I(\theta', \phi')$ also defined on the surface of a sphere centre O but with the primed coordinate system tilted relative to the unprimed coordinates by a negative rotation ψ about the common Oy axis. The angle ψ will be known as the feed tilt angle. The boundary Γ_f of the defined far-field lies on a θ-constant circle, namely $\theta = \theta_f$ and the reflector surface is bounded by the surface of the cone $\theta' = \theta'_f$. Westcott and Norris (1975, to be referred to as I), show that the reflector surface $r(\theta, \phi)$, referred to the far-field coordinates, is given by

$$r(\theta, \phi) = \tfrac{1}{2} \exp[\sigma(\theta, \phi)](1 + \sigma_\theta^2 + \sigma_\phi^2/\sin^2\theta). \tag{1}$$

σ is given by the solution of the second-order partial differential equation

$$\sigma_{\theta\theta}\sigma_{\phi\phi} - \sigma_{\theta\phi}^2 = a\sigma_{\theta\theta} + 2b\sigma_{\theta\phi} + c\sigma_{\phi\phi} + d + eD(\theta, \phi, \theta', \phi'), \tag{2}$$

in the region

$$0 \leqslant \theta \leqslant \theta_f, \qquad 0 \leqslant \phi \leqslant 2\pi,$$

where

$$D = \frac{G(\theta, \phi)}{I(\theta', \phi')} \tag{3}$$

and a, b, c, d and e are explicit functions of σ_θ, σ_ϕ and θ given by (22) of I.

Equation (2) is the elliptic form of the general equation and requires boundary conditions defined over a closed region of the far-field for its solution. In this paper two simplifications are made in order to facilitate its solution. The first is that the source is considered to radiate isotropically over the solid angle defined by the reflector surface, thus $I = I_0$, a constant over $\theta'_r \leqslant \theta' \leqslant \pi$, $0 \leqslant \phi' \leqslant 2\pi$. The second simplification requires that G, and hence D, is an even function about the Ox axis, implying that $D(\theta, \phi) = D(\theta, -\phi)$. (2) may then be solved under the following boundary conditions:

(i) $$G(\theta, \phi) = Kg(\theta, \phi), \tag{4}$$

where

$$K = 2\pi I_0(1 + \cos\theta_r)\left(\int_0^{2\pi}\int_0^{\theta_f} g(\theta, \phi)\sin\theta \, d\theta \, d\phi\right)^{-1},$$

and $g(\theta, \phi)$ is the required far-field specified to within an arbitrary multiplier. (4) arises from requiring energy conservation between the reflector solid angle, defined by $\theta'_r \leqslant \theta' \leqslant \pi$, $0 \leqslant \phi' \leqslant 2\pi$ and the corresponding far-field solid angle $0 \leqslant \theta \leqslant \theta_f$, $0 \leqslant \phi \leqslant 2\pi$.

(ii) The non-linear boundary equation

$$A\sigma_\theta^2 + B\sigma_\phi^2 + C\sigma_\theta + D\sigma_\phi + E = 0, \tag{5}$$

where A, B, C, D and E are functions of θ', θ, ϕ and ψ, and are given in equations (28) of I. (5) applies for the boundary points

$$\theta = \theta_f, \qquad 0 \leqslant \phi \leqslant 2\pi,$$
$$\theta' = \theta'_r, \qquad 0 \leqslant \phi' \leqslant 2\pi.$$

This condition ensures that points on the far-field boundary are illuminated by points on the reflector boundary.

(iii) $$\sigma_\phi(\theta, 0) = \sigma_\phi(\theta, \pi) = 0 \qquad \text{for all } \theta \text{ in } (0, \theta_f), \tag{6}$$

which follows from the even azimuthal symmetry of G.

(iv) $$\sigma_\theta(\theta_f, 0) = \cot\tfrac{1}{2}(\theta_f + \psi \mp \theta'_r), \tag{7}$$

is the 'mapping directive' equation. When the upper sign is assumed an edge ray links the 'top' of the reflector with the 'top' of the far-field and for the lower sign the 'top' of the reflector is linked by an edge ray to the 'bottom' of the far-field. (7) is in fact derived directly from equations (5) and (6) in I but must be specifically included in order to resolve the ambiguity in sign.

(v) $$\sigma(0, \phi) = 0 \tag{8}$$

which assigns a reference level to $\sigma(\theta, \phi)$ without which it is only determined to within an arbitrary constant.

3. Linearization

The solution of (2), under the boundary conditions given by equations (4) to (8), may be obtained by linearizing the non-linear equations under the assumption of an approximate solution, and then applying a finite difference model to the linearized form. A system of linear simultaneous equations results, which on solution, should yield a better approximation to σ. By repetition of the process convergence to any required accuracy may be obtained. The availability of computer programs that rapidly invert the large sparse matrices obtained by this method make this approach attractive.

The linearization procedure is most simply described by representing the non-linear equations in operator form,

$$P(\sigma) = 0 \tag{9}$$

therefore

$$P(\sigma - \sigma_0 + \sigma_0) = 0, \tag{10}$$

and if σ_0 is a close approximation to the solution of equation (9), then (10) may be expanded to

$$P(\sigma) = P(\sigma_0) + P'(\sigma_0)(\sigma - \sigma_0) + \epsilon_1, \tag{11}$$

where $P'(\sigma_0)$ is the Fréchet derivative of P at σ_0 and ϵ_1 contains terms of higer order in $(\sigma - \sigma_0)$. See, for example, Rall (1969).

Defining σ_1 by the relation

$$P'(\sigma_0)(\sigma_1 - \sigma_0) = P'(\sigma_0)(\sigma - \sigma_0) + \epsilon_1, \tag{12}$$

it is seen that (11) may be rewritten in the form

$$P(\sigma_0) + P'(\sigma_0)(\sigma_1 - \sigma_0) = 0, \tag{13}$$

which is a linear equation in σ_1, and providing ϵ_1 is sufficiently small, σ_1 will be a better approximation to σ than σ_0. (12) implies that

$$P(\sigma_1) - O(\Delta\sigma^2) = 0, \tag{14}$$

where $\Delta\sigma = \sigma_1 - \sigma_0$, and is in a convenient form for the linearization of equations (2) and (5).

By rewriting (13) in the following form:

$$\sigma_1 = \sigma_0 - [P'(\sigma_0)]^{-1} P(\sigma_0),$$

where $[P'(\sigma_0)]^{-1}$ is the inversion of the linear operator $P'(\sigma_0)$, it is seen that a direct comparison can be made with Newton's iterative equation for finding successive approximations to a root of $f(x) = 0$, namely

$$x_{k+1} = x_k - [f(x_k)/f'(x_k)]$$

where x_k denotes the values from the kth iteration.

It is a simple but tedious matter to linearize equation (2) under equation (14). Explicitly, σ is replaced with $\sigma_0 + \Delta\sigma$ in equation (2), thus obtaining $P(\sigma_0 + \Delta\sigma)$. Then, ignoring terms of $O(\Delta\sigma^n)$, $n > 1$, and replacing $\Delta\sigma$ with $\sigma_1 - \sigma_0$, the final linearized form may be obtained. As an example, consider the Monge–Ampère term

$$P_m = \sigma_{\theta\theta}\sigma_{\phi\phi} - \sigma_{\theta\phi}^2$$

σ is replaced by $\sigma_0+\Delta\sigma$, which on multiplication yields

$$P_m^{k+1}=\sigma_{\theta\theta}^k\sigma_{\phi\phi}^k+\Delta\sigma_{\theta\theta}\sigma_{\phi\phi}^k+\Delta\sigma_{\phi\phi}\sigma_{\theta\theta}^k-(\sigma_{\theta\phi}^k)^2-2\Delta\sigma_{\theta\phi}\sigma_{\theta\phi}^k+O(\Delta\sigma^2).$$

Replacing $\Delta\sigma$ with $\sigma_1-\sigma_0$ the linearized form P_{ml} is obtained:

$$P_{ml}^{k+1}=\sigma_{\phi\phi}^k\sigma_{\theta\theta}^{k+1}+\sigma_{\theta\theta}^k\sigma_{\phi\phi}^{k+1}-2\sigma_{\theta\phi}^k\sigma_{\theta\phi}^{k+1}-\sigma_{\theta\theta}^k\sigma_{\phi\phi}^k+(\sigma_{\theta\phi}^k)^2.$$

The final linearized form of (2) may be written as

$$\alpha_1\sigma_{\theta\theta}^{k+1}+2\alpha_2\sigma_{\theta\phi}^{k+1}+\alpha_3\sigma_{\phi\phi}^{k+1}+\alpha_4\sigma_\theta^{k+1}+\alpha_5\sigma_\phi^{k+1}+\alpha_6=0 \tag{15}$$

where k refers to the values from the kth iteration and $\alpha_1\ldots\alpha_6$ are given in the appendix.

Similarly, the non-linear boundary condition, equation (5), may be linearized yielding

$$\sigma_\theta^{k+1}(2A\sigma_\theta^k+C)+\sigma_\phi^{k+1}(2B\sigma_\phi^k+D)-A(\sigma_\theta^k)-B(\sigma_\phi^k)^2+E=0, \tag{16}$$

where A, B, C, D and E have been previously defined.

4. The finite difference scheme

The appearance of $\sigma_{\theta\phi}$ in equation (15) necessitates the use of a nine-point molecule as the simplest finite difference structure that may be used (see, for example Ames 1965). The natural geometry of the problem lends itself well to the use of a polar grid, especially as the boundary lies on a constant θ circle. Also, the symmetry about the Ox axis reduces the grid boundary from circular to semicircular thus halving the number of equations to be solved. The finite difference structure is illustrated in figure 2.

Application of Taylor's theorem enables the following approximations to be derived for the various derivatives at the point (i, j):

$$\begin{aligned}
&\sigma_{\theta\theta}\simeq(\sigma_{i+1,j}-2\sigma_{i,j}+\sigma_{i-1,j})/\delta\theta^2,\\
&\sigma_{\phi\phi}\simeq(\sigma_{i,j+1}-2\sigma_{i,j}+\sigma_{i,j-1})/\delta\phi^2,\\
&\sigma_{\theta\phi}\simeq(\sigma_{i+1,j+1}-\sigma_{i+1,j-1}-\sigma_{i-1,j+1}+\sigma_{i-1,j-1})/4\delta\theta\delta\phi,\\
&\sigma_\theta\simeq(\sigma_{i+1,j}-\sigma_{i-1,j})/2\delta\theta,\\
&\sigma_\phi\simeq(\sigma_{i,j+1}-\sigma_{i,j-1})/2\delta\phi,
\end{aligned} \tag{17}$$

where $\delta\theta$ and $\delta\phi$ are the incremental angles between adjacent points.

By substituting the expressions in equations (17) for the derivatives in equation (15), a nine-term linear difference equation in $\sigma_{i,j}$ results for all interior points $(i=2\ldots i_{max}-1, j=2\ldots j_{max}-1)$. For the points $(i=2\ldots i_{max}-1, j=1$ and $j_{max})$ the symmetry condition (6) is linked to (15), thus simplifying it, in that $\sigma_\phi=0$ and hence $\sigma_{\theta\phi}=0$. Also, because of the symmetry, terms in the finite difference form of $\sigma_{\phi\phi}$ (equation (17)) that lie outside the grid are replaced by their image points. Thus, $\sigma_{i,j_{max}+1}=\sigma_{i,j_{max}-1}$.

For the points $(i=i_{max}, j=2\ldots j_{max})$, the linearized boundary condition, equation (16), has to be satisfied. σ_ϕ may still be approximated by the form given in (17) but σ_θ

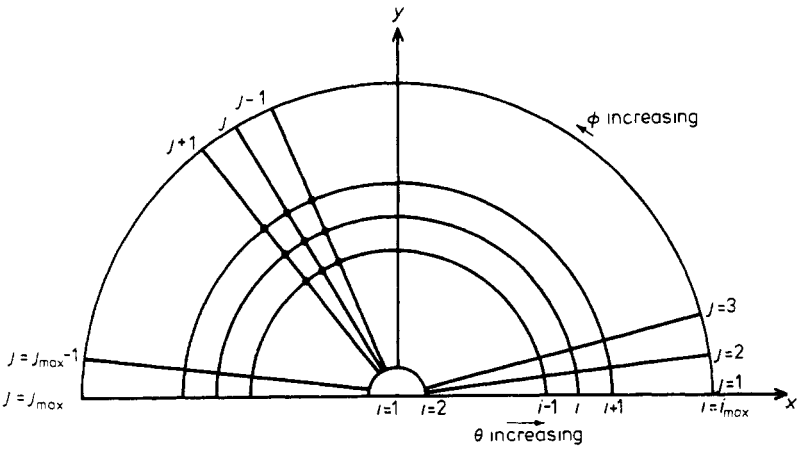

Figure 2. Finite difference scheme.

must now be represented by the backward difference formula

$$\sigma_\theta \simeq (\sigma_{i_{\max}-2,j} - 4\sigma_{i_{\max}-1,j} + 3\sigma_{i_{\max},j})/2\delta\theta.$$

The mapping directive equation (equation (7)) is applied at $(i = i_{\max}, j = 1)$. The grid point at $i = 1$ lies at a singularity in the coordinate system and hence the derivatives in ϕ are undefined at this point. However, difficulties are resolved by noting that (2) depends only on the derivatives of σ, and not on σ itself, hence an arbitrary constant may be added to any solution and the equation will still be satisfied. It is necessary therefore to assign a particular value to σ at any one point on the grid and thus (8) sets $\sigma_{1,j}$, the centre point, to zero.

The problem is reduced to solving a system of $(i_{\max}-1)\times j_{\max}$ independent linear equations in $\sigma_{i,j}$ $(i = 2 \ldots i_{\max}, j = 1 \ldots j_{\max})$, and may be solved by well known matrix methods.

In practice a modification has to be made to the scheme in order to overcome minor discontinuities that arise in the computed reflector surfaces. These occur at, and close to, the point on the surface that corresponds to the far-field pole at $\theta = 0$, and arise from the fact that surrounding points, although geometrically close, have relatively loose 'ties' with each other in the solution matrix. Errors introduced by the discretization process tend to produce differing effects on each of these elements and thus discontinuities are caused.

In order to overcome this effect stronger 'ties' may be made by explicitly incorporating the identities:

$$\sigma_\theta(0, \phi) = -\sigma_\theta(0, \phi + \pi), \qquad \sigma_{\theta\theta}(0, \phi) = \sigma_{\theta\theta}(0, \phi + \pi),$$

which, due to the symmetry of the problem, may be written as

$$\sigma_\theta(0, \phi) = -\sigma_\theta(0, \pi - \phi); \qquad 0 \leqslant \phi < \pi/2,$$
$$\sigma_\theta(0, \phi) = 0; \qquad \phi = \pi/2,$$
$$\sigma_{\theta\theta}(0, \phi) = \sigma_{\theta\theta}(0, \pi - \phi); \qquad 0 \leqslant \phi \leqslant \pi/2.$$

Approximating the derivatives by three-term forward difference formulae these equations break down to the following difference form:

$$\left.\begin{aligned} 4\sigma_{2,j} - \sigma_{3,j} &= \sigma_{3,j_{max}+1-j} - 4\sigma_{2,j_{max}+1-j} \\ \sigma_{3,j} - 2\sigma_{2,j} &= \sigma_{3,j_{max}+1-j} - 2\sigma_{2,j_{max}+1-j}, \end{aligned}\right\} j = 1 \ldots (j_{max}-1)/2.$$

$$4\sigma_{2,j} - \sigma_{3,j} = 0; \qquad j = (j_{max}-1)/2+1.$$

The relationship $\sigma_{1,j} = 0$ has been used in deriving these equations.

Since the problem is now over-specified the condition of equation (15) for the points $(i = 2, j = 1 \ldots j_{max})$ is removed. The central region is now no longer required to satisfy the differential equation and thus the resultant values of $D(\theta, \phi)$ is this region will tend to vary to some extent from the required values. Variations of up to $\pm 10\%$ have been typically encountered. However, if a better approximation to $D(\theta, \phi)$ is required in this central region slight perturbations to the computed value of K in (4) can significantly reduce the error. Generally K need be varied by only about $\pm 1\%$.

5. Computed results

The resulting sets of linear equations were solved on a CDC7600 computer using subroutines from the Nottingham Algorithms Group (NAG) FORTRAN Library (1973). Essentially a sparse matrix **A** is decomposed into triangles **A** = **LU** where **L** is lower triangular and **U** is upper triangle. An attempt is made to maintain sparsity whilst controlling round-off errors. An approximate solution to the equation **Ax** = **b** is then found by a forward and backward substitution.

A number of successful computations have been performed using a variety of far-field models, but discussion in this paper is limited to the solution of reflection surfaces for two particular far-fields, models I and II. A 154-point scheme gave satisfactory results in both cases, since σ was found to vary slowly over the integration domain. Typically maximum and minimum values of σ for these models lie between 0·2 and −0·01 respectively.

5.1. Model I

$$g(\theta, \phi) = \exp[\sin^2(3\theta)(u \sin^2\phi + v \cos^2\phi + w \cos\phi)]; \qquad 0 \leqslant \theta \leqslant 30^\circ \tag{18}$$

where $u = -2{\cdot}996$, $v = -3{\cdot}454$, $w = 1{\cdot}151$. u, v and w were chosen so that the power density at the edge of the defined field varied between 10 and 20 dB below the peak value at $\theta = 0$.

This function is represented in equi-power contours in figure 3. Several computations were made using this function, varying θ_f', the half-angle of the required reflector, and the feed tilt angle, ψ.

Solutions for both the 'top-to-top' and 'top-to-bottom' cases were obtained. For runs with $\psi = 0$ an initial guess was made for σ that would yield a reflector giving a uniform power density over the defined far-field. The equations are then ϕ independent and hence partial derivatives with respect to ϕ are zero throughout the region bounded by $\theta = \theta_f$. For this initial guess, σ may be obtained by considering only energy conservation (equation (4)) and the non-linear boundary condition, as given in equation (5). Due to the ϕ independence of this simplified problem, energy considerations alone

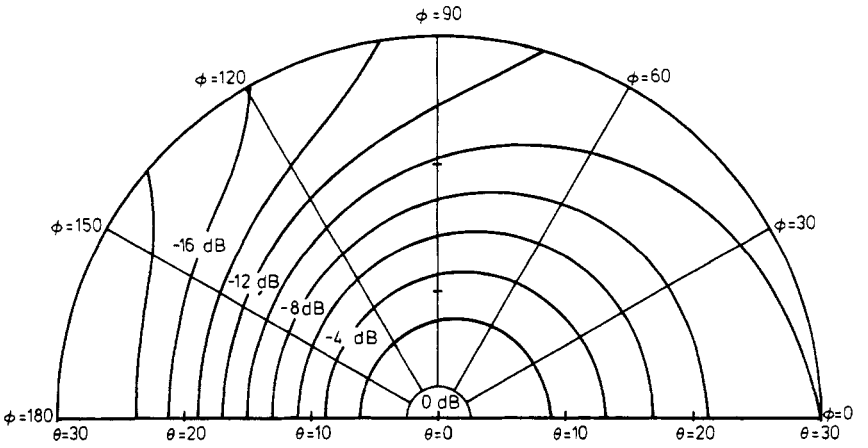

Figure 3. Model I.

define the relationship $\theta' = \theta'(\theta)$, $0 \leq \theta \leq \theta_f$. Hence, by replacing θ_f with θ, and θ_r' with θ', equation (5) may be solved directly to yield $\sigma(\theta)$.

Performing the integration in (4) under the limits $(0, \theta)$ the following relationship between θ' and θ is obtained:

$$1+\cos\theta' = A_0(1-\cos\theta),$$

where $A_0 = (1+\cos\theta_r')/(1-\cos\theta_f')$. Since $\sigma_\phi = 0$ and $\psi = 0$ equation (5) may be simplified to:

$$(\cos\theta' - \cos\theta)\sigma_\theta^2 - 2\sin\theta\,\sigma_\theta + \cos\theta' - \cos\theta = 0, \tag{19}$$

where the boundary values, θ_r' and θ_f, have been replaced by the general points θ' and θ. Equation (19) is quadratic in σ_θ and hence

$$\sigma_\theta = \frac{\sin\theta \mp \sin\theta'}{\cos\theta' - \cos\theta} = \cot\tfrac{1}{2}(\theta \pm \theta'), \tag{20}$$

which may be solved numerically to yield σ. The upper sign in (20) applies to the 'top-to-bottom' mapping and the lower sign to the 'top-to-top'.

Using this initial approximation for σ with the far-field given by (18), convergence to a stable solution for reflectors with an included angle of up to 160° was obtained in about 5 iterations.

When a feed tilt was introduced to avoid feed blockage, it was found necessary to increase ψ in steps of about 10° using the solution for $\psi - 10°$ as the initial approximation. Attempts at larger jumps in ψ resulted in the method becoming unstable. Figure 4 illustrates a cross section of the reflector surface by a cut in the $\phi' = 0$, 180° plane for the case $\psi = 0$. The solutions for both the top-to-top and the top-to-bottom variants are shown together with the resulting edge rays. Figure 5 shows the same cut through the surface but the design feed tilt angle has been changed to $\psi = 40°$. From the ray diagram it is seen that for this value of ψ, feed blockage is completely removed.

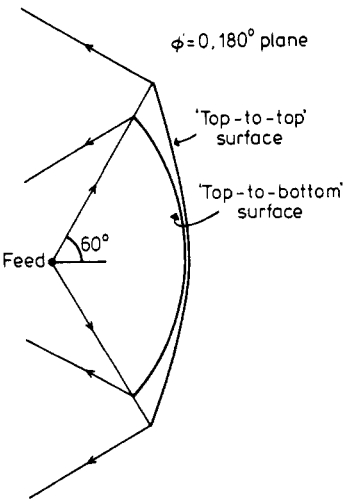

Figure 4. Showing the two possible solutions in the elliptic case.

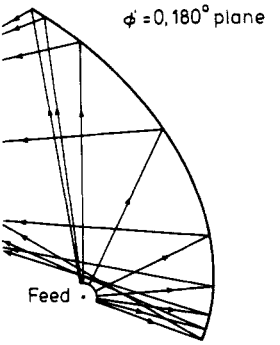

Figure 5. Reflector surface with zero feed blockage. Reflected rays lie in equal increments of θ.

5.2. Model II

$$g(\theta, \phi) = \frac{\cos(8 \sin(a_0\theta)\sin\phi)}{\sin^2(\sin(a_0\theta)\cos\phi - b_0)}; \qquad 0 \leqslant \theta \leqslant 40°,$$

where $a_0 = 0{\cdot}239$ and $b_0 = 0{\cdot}236$ which essentially results in a $(\text{cosec})^2$ shaping in $y =$ constant planes and a cosine shaping in $x =$ constant planes. An equi-power contour diagram for this function is given in figure 6. Again a satisfactory initial approximation was found to be the uniform far-fieid case and convergence was obtained in 5 iterations. Figure 7 illustrates the reflector surface obtained for the $\psi = 0$ case at cuts of $\phi' = 0$, 180° and $\phi' = 90°$, 270°. No difficulty was experienced when ψ was increased to remove feed blockage.

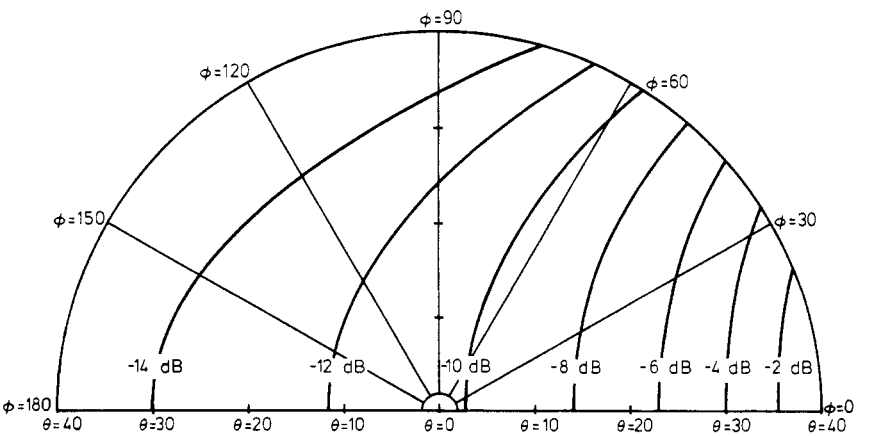

Figure 6. Model II.

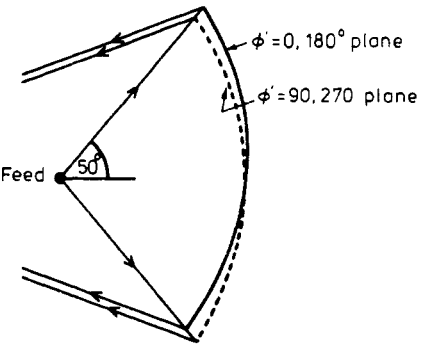

Figure 7. Model II reflector.

6. Conclusions

A method based on new design equations derived under the geometrical optics approximation has been presented for the computation of reflector surfaces that produce a given far-field radiation pattern, specified as a function of two variables. The primary feed has been assumed to behave as a point source, having an isotropic radiation pattern over the solid angle subtended by the reflector. Examples have been given illustrating two distinct classes of reflectors that may be obtained, which depend on the required mapping of the edge rays. It is also shown that the source may be positioned such that it does not lie in the path of reflected rays so that feed blockage is removed. A future paper will present a modification of the method of solution which will enable a primary source with a tapered illumination pattern to be used. The low-edge illumination of the reflector that is possible by using such a feed will enhance the practical beam shape compared to the isotropic feed, by lowering both the expected diffraction ripple across the beam and the sidelobe structure. Use of a conical scalar feed horn as the primary source, with its inherently low integrated cancellation ratio will make the technique highly suitable for applications that require good circular polarization performance.

Appendix

$$\alpha_1 = \tfrac{1}{2}\sin^2\theta[(\sigma_\theta^k)^2 - 1] - \tfrac{1}{2}(\sigma_\phi^k)^2 - \sigma_\theta^k \sin\theta\cos\theta - \sigma_{\phi\phi}^k$$

$$\alpha_2 = (\sigma_\theta^k - \cot\theta)\sigma_\phi^k + \sigma_{\theta\phi}^k$$

$$\alpha_3 = \tfrac{1}{2}[(\sigma_\phi^k/\sin\theta)^2 - (\sigma_\theta^k)^2 - 1] - \sigma_{\theta\theta}^k$$

$$\alpha_4 = (\sin^2\theta\sigma_\theta^k - \sin\theta\cos\theta)\sigma_{\theta\theta}^k + 2\sigma_\phi^k\sigma_{\theta\phi}^k - \sigma_\theta^k\sigma_{\phi\phi}^k + \sin^2\theta\sigma_\theta^k[s + (\sigma_\theta^k)^2] + (\sigma_\phi^k)^2(\sigma_\theta^k - \tfrac{3}{2}\cot\theta) - \tfrac{1}{2}\sin\theta\cos\theta[1 + 3(\sigma_\theta^k)^2]$$

$$\alpha_5 = 2\sigma_{\theta\phi}^k(\sigma_\theta^k - \cot\theta) + \frac{\sigma_\phi^k\sigma_{\phi\phi}^k}{\sin^2\theta} + \sigma_\phi^k\left(s + t + \frac{(\sigma_\phi^k)^2}{\sin^2\theta} - \sigma_{\theta\theta}^k\right)$$

$$\alpha_6 = \sigma^k_{\theta\theta}\sigma^k_{\phi\phi} - (\sigma^k_{\theta\phi})^2 - \alpha_4\sigma^k_\theta - \alpha_5\sigma^k_\phi + \tfrac{1}{2}(\sigma^k_\phi)^2\left(t + \frac{(\sigma^k_\phi)^2}{2\sin^2\theta}\right) - \tfrac{1}{2}\sin\theta\cos\theta\,\sigma^k_\theta[1+(\sigma^k_\theta)^2]$$

$$-\tfrac{1}{4}\sin^2\theta\left[1 - s\left(1 + (\sigma^k_\theta)^2 + \frac{(\sigma^k_\phi)^2}{\sin^2\theta}\right) - (\sigma^k_\theta)^4\right]$$

where $s = [1+(\sigma^k_\theta)^2 + (\sigma^k_\phi/\sin\theta)^2]D$ and $t = (\sigma^k_\theta - \cot\theta)(\sigma^k_\theta - 2\cot\theta)$.

Acknowledgments

One of us (APN) is indebted to the UK Science Research Council and Plessey Radar Ltd for support.

References

Ames W F 1965 *Nonlinear Partial Differential Equations in Engineering* (New York: Academic Press)
Brickell F and Westcott B S 1976 *J. Phys. A: Math. Gen.* **9** 113–28
Dunbar A S 1948 *Proc. IRE* **36** 1289–96
Galindo V 1964 *IEEE Trans. Antennas Propag.* **12** 403–8
Millington G 1975 *Proc. IEE* **122** 131–4
Norris A P and Westcott B S 1974 *Electron. Lett.* **15** 322–3
Rall L B 1969 *Computational Solution of Nonlinear Operator Equations* (New York: Wiley)
Westcott B S and Brickell F 1976 *J. Phys. A: Math. Gen.* **9** 611–25
Westcott B S and Norris A P 1975 *J. Phys. A: Math. Gen.* **8** 521–32